Available online at www.sciencedirect.com
ScienceDirect
Journal of Molecular Catalysis A: Chemical 276 (2007) 41–46
JOURNAL OF MOLECULAR CATALYSIS A: CHEMICAL
www.elsevier.com/locate/molcata

Effect of tantalum addition on anatase phase stability and photoactivity of aqueous sol–gel derived mesoporous titania

K.V. Baiju [a], P. Shajesh [a], W. Wunderlich [b], P. Mukundan [a], S. Rajesh Kumar [c], K.G.K. Warrier [a,*]

[a] *Materials and Minerals Division, National Institute for Interdisciplinary Science and Technology, Formerly Known as Regional Research Laboratory (CSIR), Thiruvananthapuram 695019, India*
[b] *Tokai University, Faculty of Engineering, Department of Material Science, Kanagawa 259-1292, Japan*
[c] *Centre for Materials for Electronic Technology, Hyderabad 500051, India*

Received 15 May 2007; accepted 18 June 2007
Available online 22 June 2007

Abstract

The effect of the addition of tantalum to nanocrystalline titania matrix on the photocatalytic activity is presented. The tantalum addition increases the anatase phase stability to above 1000 °C by inhibiting the increase in crystallite size of titania. All the tantalum added titania compositions have higher surface area than pure titania. Transmission electron micrograph images support the reduction in crystallite size of titanium oxide in presence of tantalum. Addition of tantalum above 1 mole percentage increases photocatalytic activity considerably and the activity is much higher than that of commercially available Hombikat UV 100 titania. All the compositions containing tantalum have higher photoactivity than pure titania. The synergistic effect of high surface area and small crystallite size is found to be responsible for the observed photocatalytic activity rates. The aqueous sol–gel method adopted for the preparation of tantalum added titania from cheaper salt precursors and the resultant highly photoactive titania make this investigation promising for various technological applications.

Keywords: Sol–gel; Titanyl oxysulphate; Photocatalyst; Anatase; Rutile

1. Introduction

Titania is a well known wide band gap semiconducting material with a wide range of applications. Scientific interest in titania has grown immensely followed by an explosive increase in research on this material over the last decade. The technological exploitation of this material is mainly based on its property of photoactivation [1–4]. From solar cells to medium for environmental cleanup, titania has provided the cutting edge for a range of technologies [5–7]. Mainly two aspects of photocatalytic activity of titania are looked upon, one is to increase the photocatalytic activity itself while the other is to shift the band gap to the visible region of the electromagnetic spectra [8]. Selective doping with metal ions and oxides like Cr^{3+}, Fe^{3+}, Sb^{5+}, Pt, Si^{4+}, Mo^{5+}, WO_3, La^{3+}, Eu^{3+}, Nd^{3+}, Pr^{3+}, Er^{3+}, Dy^{3+}, ZrO_2 have been successful in increasing the photoactivity to various extent [9–17]. Current literature available on tantalum doping is restricted to the change in electrical properties and a comprehensive documentation of the more important effects on photoactivity is required [18,19]. Visinescu et al. [20] correlated blue shift in band gap and crystallisation with photoactivity of sputtered tantala doped titania film. Recently, Wang et al. [21] reported the photoactivity of polymer templated titania/tantalum mixed oxide and they explain the high photoactivity of the system by considering the change in optical property and surface area of the mixed oxide system. Here we have studied the effects of tantalum addition on the photoactivity of titania and have tried to understand the influence of other parameters like surface area, crystallite size and phase assemblage on the activity.

2. Experimental

2.1. Material preparation

Titanyl oxysulphate ($TiOSO_4$, Aldrich, 99.99% purity) was used as the precurssor for the synthesis of titania sol. In a

* Corresponding author. Tel.: + 91 471 2490674; fax: +91 471 2491 712.
E-mail address: wwarrierkgk@yahoo.co.in (K.G.K. Warrier).

1381-1169/$ – see front matter © 2007 Elsevier B.V. All rights reserved.
doi:10.1016/j.molcata.2007.06.017

typical experiment, titanyl oxysulphate was dissolved in 500 ml of distilled water (0.2 M) and hydrolysed by slow addition of ammonium hydroxide (10%, S.D. Fine Chemicals, India) solution under constant stirring at room temperature (32 °C), until the pH of the reaction mixture was 8.0. The precipitate obtained was separated by filtration and was washed free of sulphate ions (confirmed by the $BaCl_2$ test) with distilled water. The precipitate was further dispersed in 1000 ml of hot distilled water and was peptised by the addition of 10% HNO_3 (Merck, India) solution. A stable sol was obtained at a pH range 1.7–2.2. Tantalum oxalate (M/s CMET, Hyderabad, AR grade, 99% purity) solution corresponding to 1, 2, 5 and 10 mole percentage of tantalum was added drop wise in separate batches of titania sol and kept under stirring for a period of 1 h. The sols were concentrated over steam bath and subsequently dried in an electric hot air oven at 70 °C to obtain the xerogel. These gels were further calcined at different temperatures between 500 and 1100 °C with a 10 °C min^{-1} ramp and soaking for 1 h at respective temperatures.

2.2. Characterisation

The surface area measurements and pore analysis were carried out by nitrogen adsorption using Micromeritics Gemini 2375 surface area analyser after degassing each sample at 200 °C for 2 h. XRD patterns of the calcined gels were taken in a Philips X' pert X-ray diffractometer in the diffraction angle 2θ range 20–60° using Cu Kα radiation. The amount of rutile in the sample was estimated using the Spurr equation [22]

$$F_R = \frac{1}{[1 + \{0.8\, I_A(1\,0\,1)/I_R(1\,1\,0)\}]}$$

where F_R is the mass fraction of rutile in the sample and I_A (1 0 1) and I_R (1 1 0) are the integrated main peak intensities of anatase and rutile, respectively. The crystallite size was calculated using Scherrer equation [23]

$$D = \frac{K\lambda}{\beta \cos\theta}$$

where K is the shape factor taken as 0.9 for the calculations presented, λ the wavelength of the X-ray, β the full width at half maxima, and θ is the diffracting angle.

The TEM observation of the calcined titania powder was performed on a Hitachi HF 2200 TU file emission microscope operating at an accelerating voltage of 200 kV.

The diffuse reflectance spectrum was measured using UV–vis spectrometer (Shimadzu, Japan, UV-2401 PC) keeping $BaSO_4$ as standard.

The photocatalytic activity of the titania with and without tantalum addition after calcination at 500 and 600 °C was studied by measuring the amount of methylene blue degraded under UV radiation. For the methylene blue degradation studies, aliquots were prepared by dispersing 0.1 g of titania powder in 250 ml of 6.4×10^{-9} mol l^{-1} methylene blue solution (AR grade, Qualigens Fine Chemicals, India). Absorption maximum between 640 and 680 nm in the UV spectrum of methylene blue was used for determining the concentration. The suspension was equilibrated by stirring in the dark for 1 h prior to measurements. To eliminate the error due to the adsorption of methylene blue by titania from the measurements the initial concentration of methylene blue was measured only after equilibration. The suspension was then irradiated with UV using a Rayonet Photoreactor (Netherlands) with constant stirring. The UV source was fifteen 15 W tubes (Philips G15 T8) arranged in circular fashion emitting radiation in the region 200–400 nm. The degradation of the dye was monitored using a UV–vis spectrometer (Shimadzu, Japan, UV-2401 PC). A blank dye solution was also irradiated, for about 1 h to confirm that the dye was not photobleached by the radiation in the UV chamber.

3. Results and discussions

3.1. XRD analysis

An aqueous sol–gel method was used for the preparation of tantalum added titania nano particles. The source of titania and tantalum were titanyl sulphate and tantalum oxalate, which are much cheaper than their alkoxide counter part. The X-ray diffraction pattern of anatase has a main peak at $2\theta = 25.2°$ corresponding to the 1 0 1 planes (JCPDS 21-1272) and the main peak of rutile phase is due to its 1 1 0 planes (JCPDS 21-1276) present at $2\theta = 27.4°$. The X-ray diffraction patterns of titania, with and with out tantalum addition, calcined at different temperatures are given in Figs. 1–3.

Considerable stability of the anatase phase is observed for the tantalum added titania samples and stability increases with increasing concentration of tantalum. Only 21% of titania is present as anatase in pure titania after calcination at 700 °C, while it is 88% in presence of 5 mol% tantalum added titania. Significant is the case for 10 mol% tantalum added titania where no phase transformation is observed. Pure titania completely transforms to rutile at 800 °C, while complete transformation occurs only above 1000 °C for the 10 mol% tantalum added tita-

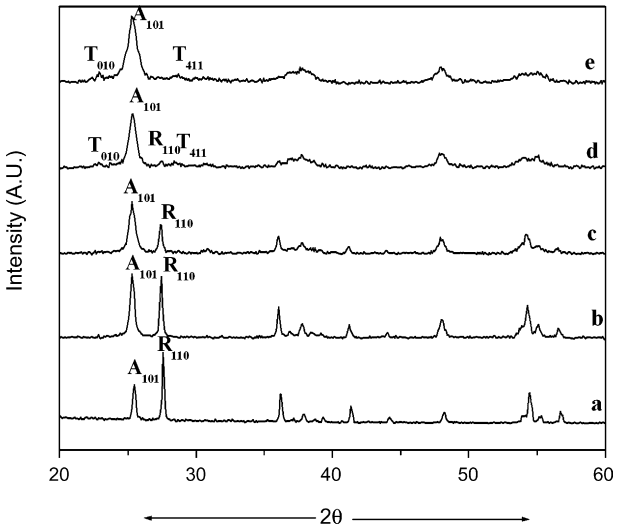

Fig. 1. XRD patterns of different TiO_2 samples calcined at 700 °C for 1 h: (A) Anatase, (R) Rutile (T) Ta_2O_5. (a) Pure TiO_2, (b) 1 mol% Ta_2O_5 added TiO_2, (c) 2 mol% Ta_2O_5 added TiO_2, (d) 5 mol% Ta_2O_5 added TiO_2, and (e) 10 mol% Ta_2O_5 added TiO_2.

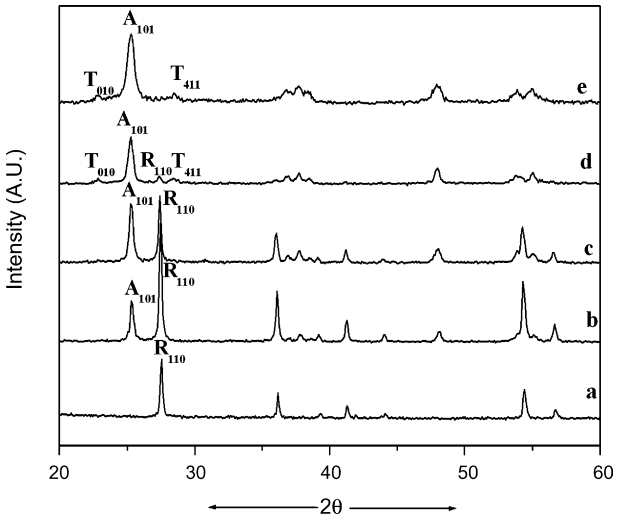

Fig. 2. XRD patterns of different TiO_2 samples calcined at 800 °C for 1 h: (A) Anatase, (R) Rutile (T) Ta_2O_5. (a) Pure TiO_2, (b) 1 mol% Ta_2O_5 added TiO_2, (c) 2 mol% Ta_2O_5 added TiO_2, (d) 5 mol% Ta_2O_5 added TiO_2, and (e) 10 mol% Ta_2O_5.

nia, indicating the high order of thermal stability of the anatase phase. The fraction of rutile phase present at different temperatures for the different samples is given in Fig. 4. X-ray diffraction patterns indicate the presence of small peaks corresponding to orthorhombic Ta_2O_5 (JCPDS 79-1375) in the compositions containing 5 and 10 mol% tantalum added titania.

3.2. BET surface area analysis

Textural characteristics of the samples calcined at 500, 600 and 800 °C was derived from N_2-adsorption analysis. The adsorption isotherms (see Supplementary data) of all samples show type IV behaviour with the characteristic hysterisis loop

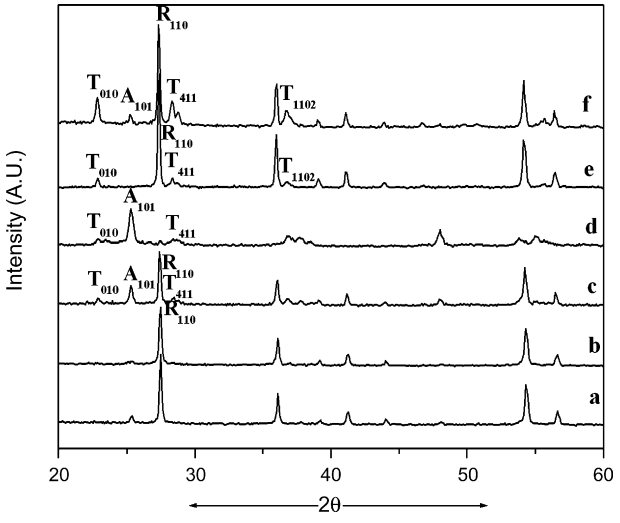

Fig. 3. XRD patterns of different TiO_2 samples calcined at different temperatures: (A) Anatase, (R) Rutile (T) Ta_2O_5 (a) 1 mol% Ta_2O_5 added TiO_2, (b) 2 mol% Ta_2O_5 added TiO_2, (c) 5 mol% Ta_2O_5 added TiO_2, (d) 10 mol% Ta_2O_5 added TiO_2 calcined at 900 °C, (e) 5 mol% Ta_2O_5 added TiO_2, and (f) 10 mol% Ta_2O_5 added TiO_2 calcined at 1000 °C.

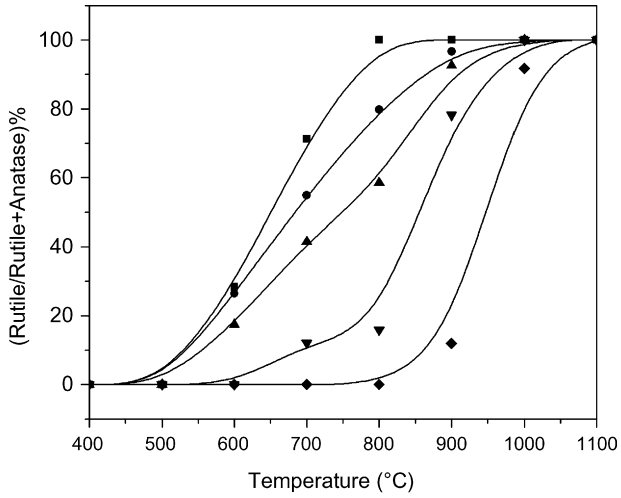

Fig. 4. Phase transformation from anatase to rutile of pure and Ta_2O_5 added TiO_2 calcined at different temperatures for 1 h. (■) Pure TiO_2, (●) 1 mol% Ta_2O_5 added TiO_2, (▲) 2 mol% Ta_2O_5 added TiO_2, (▼) 5 mol% Ta_2O_5 added TiO_2, and (♦) 10 mol% Ta_2O_5.

[24]. The mesoporous nature of the titania samples is evident. The surface area obtained for tantalum added samples are much higher than that obtained for pure titania at all calcined temperatures. The surface area obtained for pure and tantalum added titania samples calcined at different temperatures are plotted in Fig. 5. The surface area of the samples follows the same trend at all calcined temperatures. There is an increase in surface area for up to 2% addition and beyond which a decline is observed. But even for 10% tantalum addition the surface area is higher than that of pure titania.

3.3. UV spectral analysis

The electronic bands of different titania samples were studied using UV–vis/diffuse reflectance spectroscopy. The obtained spectra are provided in Fig. 6. All the samples show bands around 300–350 nm characteristic of segregated crystallites of anatase

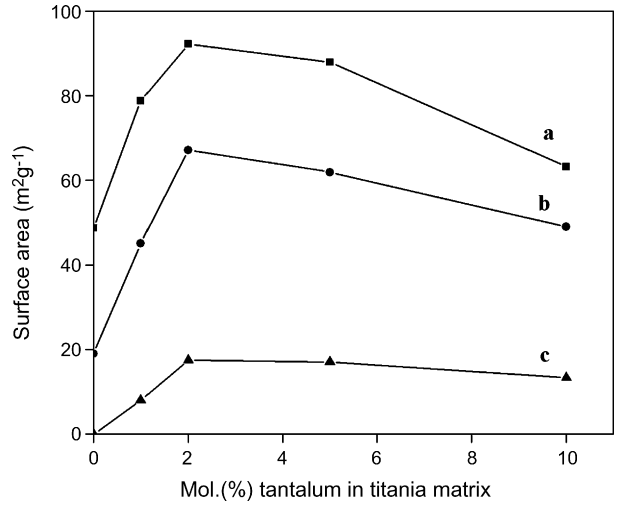

Fig. 5. Surface area vs. concentration of tantala of pure and tantala added titania at (a) 500 °C, (b) 600 °C and (c) 800 °C.

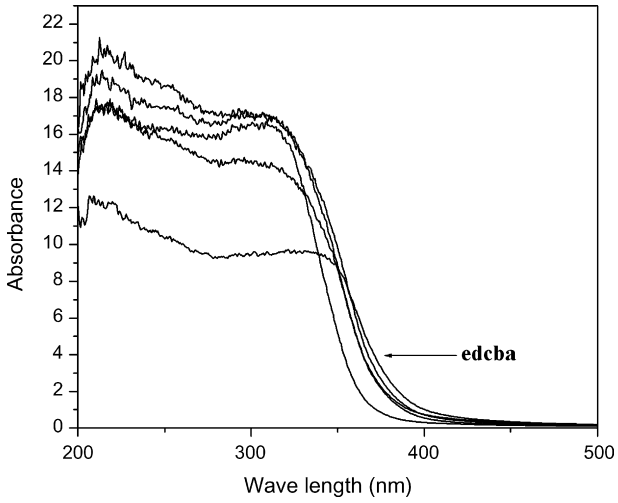

Fig. 6. DRS spectrum of TiO_2 samples calcined at 500 °C for 1 h. (a) Pure TiO_2, (b) 1 mol% Ta_2O_5 added TiO_2, (c) 2 mol% Ta_2O_5 added TiO_2, (d) 5 mol% Ta_2O_5 added TiO_2, and (e) 10 mol% Ta_2O_5 added TiO_2.

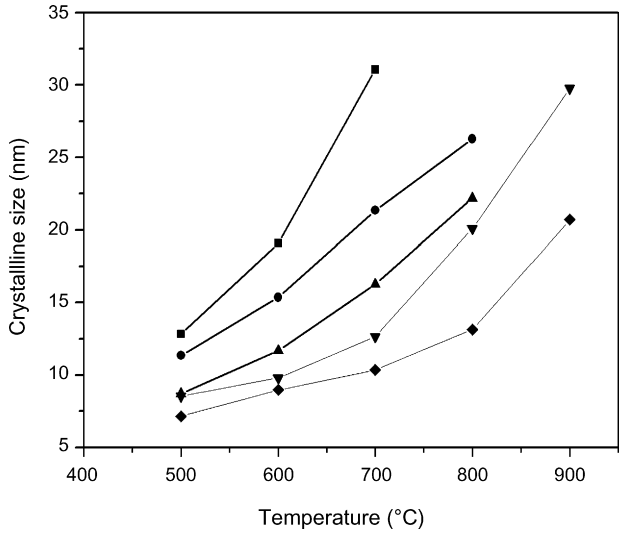

Fig. 7. Crystallite size of the anatase phase in pure and Ta_2O_5 added TiO_2 calcined at different temperatures for 1 h. (■) Pure TiO_2, (●) 1 mol% Ta_2O_5 added TiO_2, (▲) 2 mol% Ta_2O_5 added TiO_2, (▼) 5 mol% Ta_2O_5 added TiO_2, and (♦) 10 mol% Ta_2O_5 added TiO_2.

[25]. It can be seen that increasing the concentration of tantalum in the titania matrix results in absorption starting from a lower wavelength region, i.e. UV–vis absorption spectra shows a 'blue shift' in the absorbance onset value in the case of tantalum added titania. There is a significant shift in absorbance onset value for the 10 mol% tantala added sample. The phenomenon of blue shift of absorbance onset values is observed for semiconducting systems when the domain size reaches nano regimes where quantum size effects start to get pronounced [26].

3.4. Crystallite size determination

The crystallite size obtained for the different titania samples are given in Fig. 7. The crystallite size can be seen to decrease with increasing tantalum concentration. The blue shift in the band edge is hence due to the quantum size effects resulting from the smaller size of anatase crystallites as a result of the progressive tantalum addition. The TEM images of pure and 10 mol% tantalum added titania samples, presented in Fig. 8a and b show that pure titania has a crystallite size of 23 nm and 10 mol% tantalum added titania has a crystallite size of 6 nm and confirms the quantum size effects reasoned above.

The crystallite sizes plotted as a function of temperature reveal that the progressive tantalum addition hinders the growth of anatase titania. Thermodynamic stability of anatase phase compared to rutile in smaller crystallites is a well known phenomenon and hence the increased stability of the anatase phase observed here is due to the restriction in crystallite growth imposed by tantalum.

3.5. Photoactivity studies

The photocatalytic activity of the titania samples calcined at 500 °C tested against methylene blue degradation is given in Fig. 9. Photo degradation of methylene blue on titania surface follows a first order rate equation [27,28]. Hence, a linear fit to the plots of $\log(c_0/c)$ against time was done using origin 7 software. The increase in tantalum content increases the activity of titania as evident from the graph. There is a considerable shift

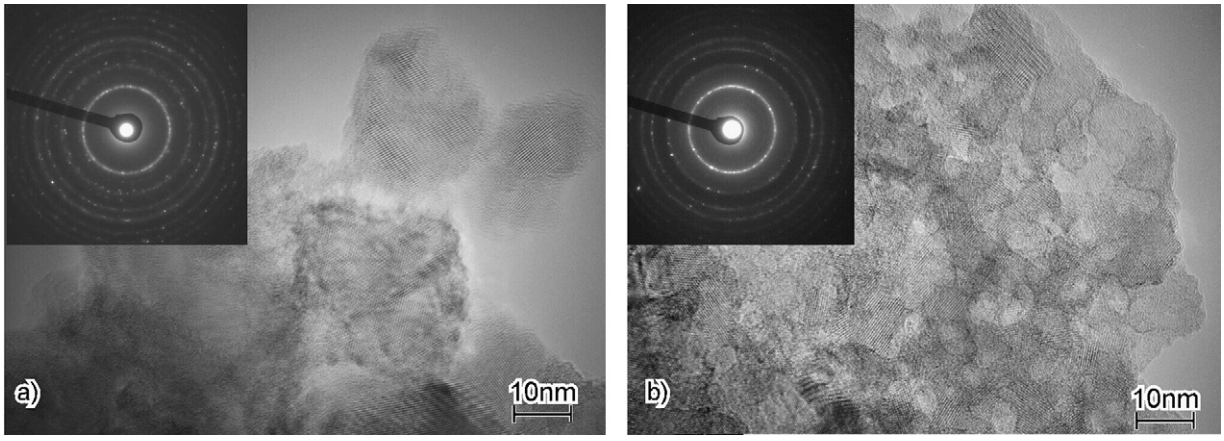

Fig. 8. TEM images of (a) TiO_2 sample at 600 °C and (b) 10 mol% Ta_2O_5 added TiO_2 at 600 °C.

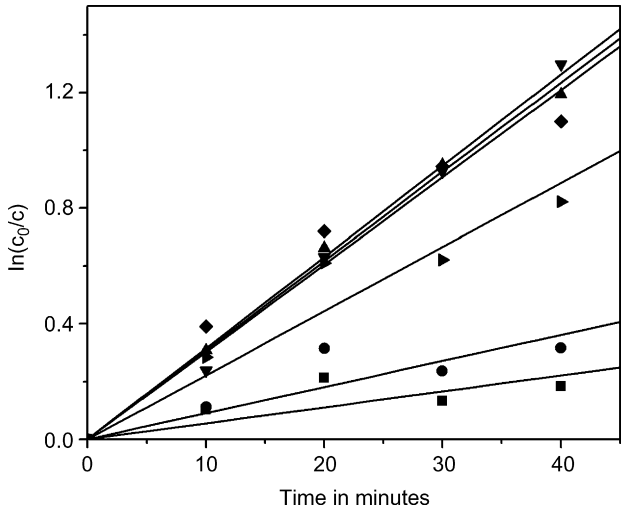

Fig. 9. Photocatalytic degradation profile of pure and tantalum added titania calcined at 500 °C. (■)Pure TiO_2, (●)1 mol% Ta_2O_5 added TiO_2, (▲)2 mol% Ta_2O_5 added TiO_2, (▼)5 mol% Ta_2O_5 added TiO_2, and (♦)10 mol% Ta_2O_5 added TiO_2. (►) Hombikat UV 100 TiO_2.

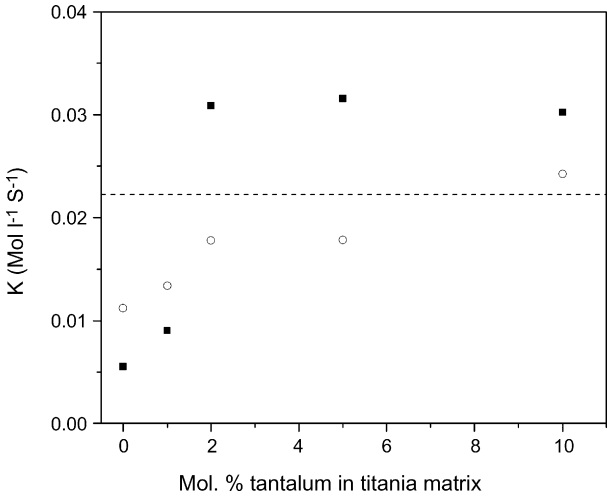

Fig. 10. The rate constants for the samples calcined at (■) 500 °C and (○) 600 °C are plotted against the percentage of tantalum. Rate constant obtained for Hombikat UV 100 is shown as the dashed line.

in rate when concentration of tantalum is increased from 1 to 2 mol%. Further increase in photoactivity with tantalum content is not that pronounced. In fact a slight decrease is observed for the 10 mol% tantala added titania. For comparison of activity a commercially available titania sample, Hombikat UV 100 is also tested. Addition of tantalum above 1 mol% gives titania with much better activity than commercially available Hombikat UV 100 titania.

The addition of tantalum into titania matrix increases the anatase phase stability. Increasing addition of tantalum seems to result in the segregation of tantalum oxide as evidenced by the appearance of its peaks in the XRD [JCPDS 79-1375]. This in disagreement with the observation of Sacerdoti where they could not find any peaks related to tantalum oxide in their XRD patterns [29]. But there is a significant difference in the preparation procedures adopted. While we have used salt precursors for both tantalum and titania they had chosen all alkoxide precursors. The decrease in crystallite size is a common observation and considering the comparable ionic radii of tantalum (0.064 nm) and titanium ions (0.061 nm) we conclude that substitution of titanium ions by tantalum ions takes place for all concentrations. Increasing concentration leads to segregation of tantala. In either case the stability of anatase phase is increased progressively.

Precursor gel calcined at 500 °C has only anatase phase for all samples including pure titania. Hence, the ratio of anatase to rutile phase can be ruled out as influencing the photocatalytic activity. The slope for the plots of $\log(c_0/c)$ versus time gives the rate constants for the first order reaction. The rate constants for the samples calcined at 500 and 600 °C are plotted against the percentage of tantalum in Fig. 10. The difference in surface area alone will not be able to account for the observed trend. For the 500 °C calcined sample, the 2% tantala added titania has a surface area of 92 $m^2\ g^{-1}$ and has activity three times than that of the 1 mol% tantalum added titania which has a surface area of 78.8 $m^2\ g^{-1}$. At the same time the 10 mol% tantala added titania has a surface area of only 63 $m^2\ g^{-1}$ but has activity close to that of the 2 mol% tantala added titania. When calcined at 600 °C for compositions below 2 mol% tantalum addition there is an increase in activity but for samples with 2 mol% tantala and above there is significant decrease in activity. Even for the 1 and 2 mol% tantala added titania the surface area decreases but the activity can be seen to increase by about an order in magnitude.

Table 1 provides the samples tested in the decreasing order of their activity. Crystallite size, surface area and rutile fraction in the sample are all provided for clarity of discussion. From the table it can be seen that the samples with high activity has either crystallite size below 9 nm or has a mixture of phases.

Table 1

Sample	Calcination temperature	Crystallite size	Surface area	Percentage rutile	Rate ($mol\ l^{-1}\ s^{-1}$)
5% Ta added TiO_2	500	8.5	87.9	0	0.03157
2% Ta added TiO_2	500	8.71	92.2	0	0.03085
10% Ta added TiO_2	500	7.15	63.2	0	0.03022
10% Ta added TiO_2	600	8.96	49	0	0.0242
2% Ta added TiO_2	600	11.66	67.1	17	0.0178
5% Ta added TiO_2	600	9.8	61.9	0	0.01782
1% Ta added TiO_2	600	15.4	45.1	26	0.0134
Pure TiO_2	600	19.08	19.1	28.35	0.01118
1% Ta added TiO_2	500	11.35	78.8	0	0.00904
Pure TiO_2	500	12.8	48.7	0	0.00553

In the absence of rutile phase high activity is observed when crystallite size falls below 9 nm. But when rutile phase is present the activity is influenced by the composition of phases along with surface area. It can be seen that there is an increase in surface area along with the increase in activity and similarly a decrease in rutile percentage.

The decrease in crystallite size in the nano regime is associative with a blue shift in absorption edge and this has been found to aid photoactivity by decreasing the rate of recombination of hole electron pairs formed by photon irradiation [30]. Mixture of rutile and anatase phase has been reported to show better activity than phase pure anatase titania. But from this study it is clear that anatase phase in the nano regime is better than a mixture of anatase and rutile phases. Tantalum addition influences the photoactivity of pure titania through a synergistic contributions from a modified phase composition, surface area and crystallite size.

4. Conclusion

An aqueous sol–gel method was used for the preparation of nanocrystalline tantala added titania. Tantalum addition increases the phase stability of anatase by restricting the growth of anatase crystallites. The TEM of pure and tantalum added titania were 23 and 6 nm respectively after calcination at 600 °C. Tantalum addition is found to increase the photocatalytic activity of titania and addition of tantala above 1 mol% and calcination at 500 °C results in titania photocatalysts with better activity than commercially available Hombikat UV 100 titania. Decrease in crystallite size is the determining factor for photoactivity in phase pure anatase samples where as rutile to anatase ratio is more important in mixed phase systems resulting from tantalum doping.

Appendix A. Supplementary data

Supplementary data associated with this article can be found, in the online version, at doi:10.1016/j.molcata.2007.06.017.

References

[1] A. Fujishima, K. Hashimoto, T. Watanabe, TiO_2 Photocatalysis Fundamentals and Applications, BKC Inc., Tokyo, 1999.
[2] W.J. Stark, K. Wegner, S.E. Partsinis, A. Baiker, L. Catal. 197 (2001) 182.
[3] M.A. Fox, M.T. Dulay, Chem. Rev. 93 (1993) 341.
[4] M. Fujihira, Y. Satch, T. Osa, Nature 293 (1981) 206.
[5] M. Gratzel, Nature 414 (2001) 338.
[6] Y. Inel, D. Ertek, J. Chem. Soc. Faraday Trans. 89 (1993) 129.
[7] D.F. Ollis, E. Pelizzetti, N. Serpone, Environ. Sci. Technol. 25 (1991) 1523.
[8] S.U.M. Khan, M. Al-Shahry, W.B. Ingler, Science 297 (2002) 2243.
[9] S. Karvinen, R.-J. Lamminmaki, Solid State Sci. 5 (2003) 1159.
[10] J.A. Navio, M. Macias, M. Gonzalez-Catalass, A. Justo, J. Mater. Sci. 27 (1992) 3036.
[11] J. Moon, H. Takagi, Y. Fujishiro, M. Awano, J. Mater. Sci. 36 (2001) 949.
[12] M. Anpo, M. Takeuchi, J. Catal. 216 (2003) 505.
[13] K.Y. Jung, S.B. Pask, Appl. Catal. B Environ. 25 (2000) 249.
[14] K. Wilke, H.D. Breuer, J. Photochem. Photobiol.: Chem. 121 (1999) 49.
[15] A. Rampaul, I.P. Parkin, S.A. O'Neill, J. Desouza, A. Mills, N. Elliott, Polyhedron 22 (2003) 35.
[16] Y. Wang, H. Cheng, L. Zhang, Y. Hao, J. Ma, B. Xu, W. Li, J. Mol. Catal. A: Chem. 151 (2000) 205.
[17] Y. Zhang, H. Xu, Y. Xu, H. Zhang, Y. Wang, J. Photochem. Photobiol. A: Chem. 170 (2005) 279.
[18] H. Lin, S. Kumon, H. Kozuka, T. Yoko, Thin Solid Films 315 (1998) 266.
[19] C. Li, J. Wang, X. Wang, H. Chen, W. Su, Mater. Chem. Phys. 74 (2002) 187.
[20] C.M. Visinescu, R. Sanjines, F. Levy, V. Marcu, V.I. Parvulescu, J. Photochem. Photobiol. A Chem. 174 (2005) 106.
[21] C. Wang, A. Geng, Y. Guo, S. Jiang, X. Qu, L. Li, J. Colloid Interface Sci. 301 (2006) 236.
[22] R.A. Spurr, H. Myers, Anal. Chim. 29 (1957) 760.
[23] W. Bai, K.L. Choy, N.H.J. Sytelzer, J. Schoonman, Solid State Ionics 116 (1999) 225.
[24] S.J. Gregg, K.S.W. Sing, Adsorption, Surface Area and Porosity, second ed., Academic Press, 1982, p. 287.
[25] A.M. Prakesh, H.M. Sung-Suh, L. Kevan, J. Phys. Chem. B 102 (1998) 857.
[26] M. Anpo, T. Shima, S. Kodama, Y. Kobokawa, J. Phys. Chem. 91 (1987) 4305.
[27] A. Houas, H. Lachheb, M. Ksibi, E. Elaloui, C. Guillard, J.-M. Herrmann, Appl. Catal. B 31 (2001) 145.
[28] Y.-H. Xu, H.R. Chen, Z.-X. Zeng, B. Lei, Appl. Surf. Sci. 252 (2006) 8565.
[29] M. Sacerdoti, M.C. Dalconi, M.C. Carotta, B. Cavicchi, M. Ferroni, S. Colonna, M.L.D. Vona, J. Solid State Chem. 177 (2004) 1781.
[30] M.A. Henderson, Surf. Sci. 400 (1998) 203.